Feasibility of using Duraform® Flex lattice structures and additive manufacturing for optimising bicycle helmet design safety

Shwe Soe*, Michael Robinson, Philip Martin, Michael Jones, Peter Theobald

Cardiff School of Engineering, Cardiff University, Queen's Buildings, The Parade, Cardiff CF24 3AA, UK
*soes@cf.ac.uk

Abstract

Bicycle helmets are designed to attenuate forces and accelerations experienced by the head during cycling accidents. An essential element of bicycle helmet design is, therefore, the appropriate manufacturing of energy dissipating components. The focus of this study was to evaluate the feasibility of using elastomeric lattice-based structures (Duraform® Flex), manufactured via a laser sintering (LS) process, as the energy dissipating inner liner of the bicycle helmet. This study is presented in two sections; the optimisation of the LS process capabilities for the manufacture of lattices based structures and an evaluation of the effects of lattice structure density on helmet impact kinematics. Through the fabrication and testing of tensile and compressive specimens, each process parameter (laser power, scanning exposure, build temperature and part orientation) was optimised to maximise compressive strength. The energy dissipating characteristics of helmet lattice structures, made from this optimised material, were evaluated during simulated helmeted headform impact tests. Reduced accelerations and increased pulse durations were reported for decreased lattice structure densities, demonstrating improved energy dissipating characteristics for this novel technique. This study demonstrates that lattice-based inner liners, manufactured via additive manufacturing processes, have exciting potential towards improving bicycle helmet safety.

1. Introduction

Head injuries are the greatest risk posed to bicyclists, comprising of approximately one-third of emergency department visits, two-thirds of hospital admissions and three-quarters of deaths associated with victims of bicycle accidents [1-6]. One important prevention strategy taken to reduce the risk of severe trauma is the use of protective cycle helmets. Wearing a protective helmet is associated with a 63-88% reduction in the risk of severe head and brain injury [7-10] and is strongly recommended by organisations including the World Health Organisation [11].

The principal purpose of a cycle helmet is to protect the head from blunt impacts that would otherwise impart large forces and accelerations to the head [12]. Cycle helmet designs consequently aim to dissipate a proportion of the impact energy,

through the use of deformable structures, to attenuate the forces and accelerations sustained by the head during a bicycle accident [12,13]. The bicycle helmet design has, essentially, remained unchanged since its successful commercial introduction in 1975 [14], with a thin, rigid, outer shell covering a thick inner liner of dense expanded foam (typically expanded polystyrene (EPS)). When impacted, the rigid outer shell structure spreads the force of the impact to distribute the transfer of impact loads to the head. Spread across a greater area, the impact proceeds to crush the inner liner to further dissipate the energy of the impact. Both features attempt to reduce the risk of cranial fractures (by reducing localised strain on the skull) and brain injury (through managing the translational acceleration of the head).

Although effective in managing translational accelerations, much controversy exists over the capability of current helmet designs to reduce rotational accelerations [15,16]. Furthermore, as the compression of the foam liner is permanent, helmets must be discarded after large impacts, as it can no longer provide adequate head protection [12,13]. Additionally, as proper helmet fit and retention is also important (an improperly fitted helmet may not provide the designed impact absorption [17]), the use of helmets principally designed for the mass market may increase the risks of trauma in certain subpopulations. Hence, in recent years researchers have recognised these drawbacks and have begun to investigate innovative concepts for improving the safety of current bicycle helmet designs [18-22].

One emerging concept is the use of additive manufacturing (AM) processes for the design and rapid manufacture of ultra-lightweight customised helmets to precisely fit the head of the consumer. Laser sintering (LS) is a promising AM process used for manufacturing 'lattice-based' structures, structures with exceptional stiffness and strength characteristics for any given weight. Such structures are typically characterised by complex geometries and can often only be fabricated via AM processes [23, 24]. Currently, scant information exists regarding LS fabricated thermoplastic elastomers, when compared to polyamides [25-27], which display some potential for use in energy absorption applications such as protective helmets.

This study implemented experimental and computational investigations to fully characterise the material properties of the thermoplastic elastomer Duraform® Flex (from 3D Systems [28]; referred to hereafter as 'Flex') and explore the potential for the adoption of this material as a customised helmet liner to, ultimately, improve the safety characteristics of commercial bicycle helmets. Hence, this study will first investigate the process capabilities for the optimisation of Flex material properties, before computationally analysing the effects of inner liner lattice structure density on helmet impact kinematics.

2 Materials and Methods

2.1 Experimental procedure

A series of tests were performed to identify the processing protocol that produces a Flex material with properties optimised for use as a protective helmet liner.

2.1.1 LS process capability for Flex material

The HiQ LS machine (3D Systems) employed in the study is fitted with a 40 W CO_2 laser and closed looped temperature control, integrated with a black body Infrared calibrator. In Table 1, the default process parameters for this material are reported alongside the adopted experimental process parameters. The unique feature of the machine operating software (version 3.45) is the capability for performing multiple scanning exposures (up to 10) in both the X and Y directions in alternate layers.

Table 1: LS process parameters – Duraform® Flex

Parameters	Default values	Experimental values
Laser power (W)	9	12-15
Scanning speed (mm/s)	5080	5080
Scan spacing (mm)	0.15	0.15
Number of scan exposures	1	1-4
Layer thickness (mm)	0.1	0.1
Powder bed temperature (°C)	153	151-156
Powder feed temperature (°C)	90	90
Roller speed (mm/s)	305	177-305
Hatch style	X and Y	X and Y

2.1.2 Build preparation

Following the manufacturer's recommendation the powder was recycled and reused in the trial builds with the minimum addition of new powder after each build. It was also notable that the maximum recommended roller speed was nearly twice that for the Duraform® Polyamide material. Trials using a lower roller speed were observed to create a lumpy powder bed and thus the maximum roller speed was maintained for all test builds.

2.1.3 Specimen fabrication

Standardised tensile testing specimens were designed in accordance with BS ISO 37:2011 (Type 1) [29], whilst standardised compression testing specimens were

designed in accordance with BS ISO 7743:2011 (Method C) [30]. To evaluate the mechanical properties of parts using different build orientations, the specimens were oriented in either the X- (horizontal) or Z-axis (vertical) of the build chamber, as shown in Figure 1. As a starting point, the trial builds were based on the default processing parameters shown in Table 1. In later builds, several key parameters such as powder bed temperature (PBT), laser power (LP) and the number of scanning exposures (NSE) were varied depending on the test results observed from the prior builds. An example of the fabricated tensile and compression test specimens are shown in Figure 2.
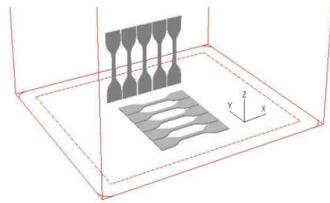
Figure 1: Build layout of tensile specimens (X-axis and Z-axis)
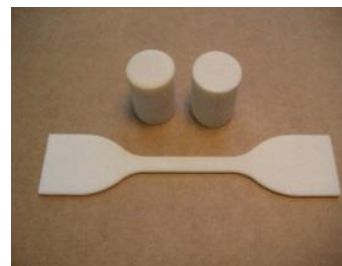
Figure 2: Fabricated tensile and compression specimens

2.1.4 Testing

Tensile testing was performed in accordance with BS ISO 37:2011 (Type 1) [29], whilst compression testing was performed in accordance with BS ISO 7743:2011 (Method C) [30]. The fabricated tensile specimens were subjected to a quasi-static loading rate of 500 mm/min, using a Shimadzu (AG-50kNG) mechanical testing machine (Shimadzu Corporation, Tokyo, Japan) and tested to failure. Compression tests were performed at a rate of 10 mm/min, with specimens compressed between platens to 25% compression. For both tests, repeated load cycles were also conducted so that the hysteresis effect and stress-softening behaviour for each cycle could be observed. During tensile testing, strain data was recorded using digital image correlation whereas for compression, the strain data was correlated from the movement of machine platen.

2.2 Computational procedure

An explicit finite element (FE) analysis was performed with Autodesk Simulation Multiphysics 2013 (Autodesk Inc., CA, USA) to analyse the energy dissipating characteristics of Flex material lattice structures during simulated helmet drop tests. To replicate a traditional helmet design, a simplified helmet was computationally modelled with two layers; a thin rigid outer shell and a thicker

energy absorbing inner liner. The thin outer shell was modelled to be 5mm thick, whilst the inner liner was modelled to be 20mm thick. As acrylonitrile butadiene styrene (ABS) plastics are commonly used for the outer shells of helmets, the outer shell was modelled with material properties analogous to ABS (E=2495MPa, G=950MPa, ρ=1151kgm^{-3}). The thicker inner liner, the principal region of interest for this analysis, was modelled using a series of simple Flex lattice structures with varying lattice densities (solid block, 5%, 10%, 15%, 20%, 25% and 30%), and an expanded polystyrene (EPS) solid block model for a comparative analyses against the material most commonly used in helmet inner liners (Figure 3). Flex material properties (assuming isotropy and hyperelasticity) were modelled by curve fitting a Moony-Rivlin model (C_1=7.559, C_2=-2.095, K=5464MPa, ρ=1018kgm^{-3}) to the stress-strain curve (Figure 4) of the optimum processed parameters (LP – 15 W and NSE – 2) described in Section 4.2. A Moony-Rivlin model was selected based on its suitability for approximating the properties of rubber-like materials [31]. All inner liners were designed with an internal radius of 50mm, whilst all lattice structures were modelled with 3mm diameter cylinders to represent the lattice densities under analysis (Figure 3). Typical low density EPS material properties (E=5.9MPa, G=2.9MPa, ρ=15.3kgm^{-3}) were extracted from the literature [32, 33].

Figure 3: The energy absorbing inner liner of helmet. Illustrated are the solid block model (left), the 25% lattice structure (middle) and the 10% lattice structure (right).

To simulate EN:BS1078 helmet impact tests [12], simplified representations of the headform and anvil were computationally modelled. The anvil was modelled by a 120x120mm steel plate (E=200GPa, G=80GPa, ρ=7872kgm^{-3}), whilst the headform was modelled by a 100mm diameter aluminium sphere (E=69GPa, G=26GPa). To represent the mass of a 10 year old child head (4.2kg [12]), the aluminium sphere was modified to have a density of 8021kgm^{-3}. The headform and both layers of the helmet were coupled via a bonded (0 degrees of freedom) joint, whilst the anvil was fully constrained along its lower surface. The bonded headform and helmet assembly (hereby referred to as the helmeted headform) was impacted on the anvil at an initial velocity of 2.2ms^{-1} and an angle acting through the centre of gravity (CG) of the helmeted headform assembly (to remove rotational accelerations). For the analysis, the differences between the simulated peak CG translational accelerations and CG translational acceleration pulse durations were compared between each inner liner design.

3. Results

3.1 Experimental data

Tables 2 and 3 describe the process parameters and properties of the tensile and compression test specimens, produced in the X and Z axes respectively. Figure 4 describes the selected compressive stress–strain properties of samples produced at LP - 15W, NSE - 2 and in the X and Z axis part build orientations.

Table 2: Process parameters and properties of tensile specimens produced in the X-axis and Z-axis

Laser power /W	No of scanning exposures	Part orientation	Tensile Strength at Break /MPa	Maximum Elongation at Break /%
12	1	X	3.1	210
12	4	X	8.9	780
12	4	Z	5.7	200
15	1	X	4.2	270
15	2	X	7.8	660
15	4	X	12.5	780
15	1	Z	0.6	30
15	2	Z	4.1	100

Table 3: Process parameters and properties of compression specimens produced in the X-axis and Z-axis

Laser power /W	No of scanning exposures	Part orientation	Strength at 25% compression /MPa
12	4	X	8.8
12	4	Z	8.5
15	2	X	8.6
15	2	Z	8.0

Figure 4: Stress-strain relationship for (left) the repeated loading cycles at 25% compression (LP: 15 W, NSE: 2, X-axis) and (right) the stabilised loading cycles at 25% compression (LP: 15 W, NSE: 2, X-axis (——) and Z-axis (– –))

3.2 Computational data

Translational accelerations were recorded from the centre of gravity of the headform for all helmet impact test simulations (Figure 5); with the exception of the 5% and 10% density Flex lattice structures, which failed to converge. When investigating the effects of lattice structure density, peak translational accelerations were decreased with a reduction in lattice structure density, whilst acceleration pulse durations were increased (Figure 6 & Table 4). These characteristics were also observed when evaluating the effects of material selection, with the Flex solid block model reducing peak translational accelerations and increasing translational acceleration pulse durations, when compared to the EPS solid block model.
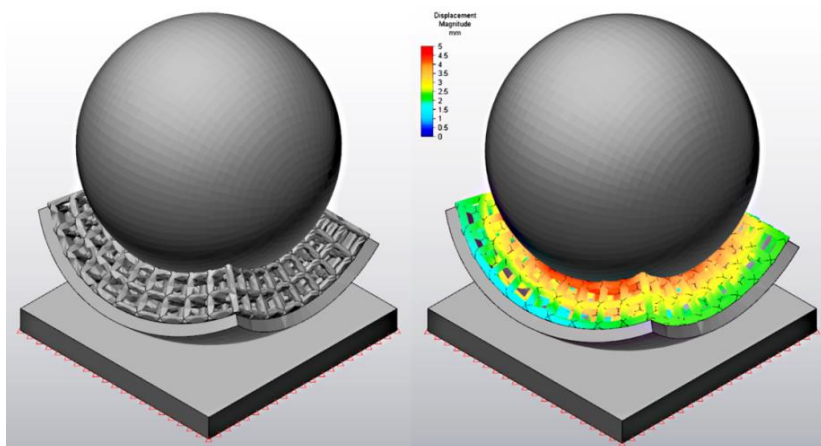
Figure 5: Finite element analysis of a helmeted headform drop test with 25% lattice insert bonded to the helmet. Presented is the finite element analysis at the moment before impact (left) and at the point of greatest deflection (right).
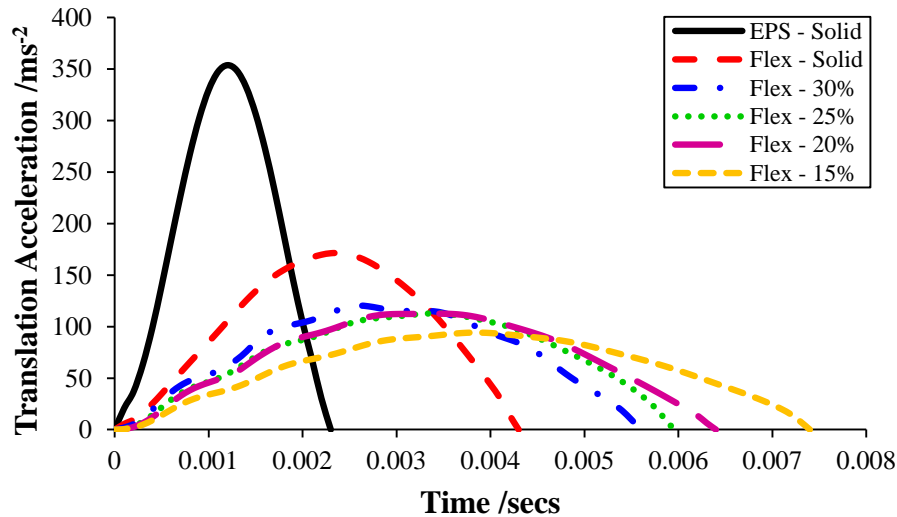
Figure 6: Effect of helmet inner liner on headform translational acceleration

Table 4: Peak translational accelerations and translational acceleration pulse durations recorded for each helmet inner liner

Inner Liner	Peak Translational Acceleration /ms^{-2} (g)	Acceleration Pulse Duration /s
EPS - Solid	354 (36)	0.0023
Flex - Solid	171 (17)	0.0043
Flex - 30%	120 (12)	0.0056
Flex - 25%	113 (12)	0.0060
Flex - 20%	113 (11)	0.0064
Flex - 15%	94 (10)	0.0074

4 Discussion

4.1 Effect of temperature

The data presented in Tables 2 and 3 and Figure 4 were collected from test builds run with a fixed PBT of 155 °C. This temperature was chosen because earlier trials at lower temperatures (such as153 °C) resulted in parts with poor tensile strength, especially in the Z-axis. In contrast, separating the parts from the hard surrounding powder proved difficult when using a PBT of 156 °C. Hence, the optimal PBT was identified (i.e. 155 °C) and maintained in all further experimental builds.

4.2 Effect of laser power, scanning exposure and part orientation

Test parts were built to assess the effect of variation in the LP, NSE and part orientation. Two different laser powers, 12 W and 15 W, were considered together with NSE up to 4.

In Table 2, selected experimental results are shown in order to highlight the similarities and differences of the end properties achievable by varying the LP and NSE. The values of Tensile Strength at Break (TS_b) and Maximum Elongation at Break (E_b) with single exposures (NSE-1) demonstrates that the parts produced at a LP of 15 W have a higher TS_b and E_b than for a 12 W LP. It can be seen in Table 2 that the TS_b and E_b increase dramatically as the NSE increases for both LPs. Specifically at 12 W, both TS_b and E_b increased about 3 times when using an NSE of 4 compared to a single exposure (NSE - 1). A similar trend can be noticed for a LP of 15 W, where the TS_b and E_b increase successively from a NSE of 1 to 2 and then to 4, although in a non-linear fashion (the increase in structural strength diminishing with increasing NSE). It also shows that the use of increased NSE has a major impact on the properties of parts built in the Z-axis. Comparison of test results for parts manufactured with NSEs of 1 and 2 at a LP of 15 W in the Z-axis, show the TS_b has increased seven times, where E_b has increased three times. The results demonstrate that the process parameters and part orientations are sensitive to tensile tests. The optimised parameters can be chosen as both the (LP: 15 W & NSE: 2) and (LP: 12 W & NSE: 4) combinations, as they provide the maximum strengths and elongations, whilst also producing the part features within acceptable tolerances. The stress-softening and hysteresis effects under repeated strain cycles exhibited in Flex parts are detailed in the prior publication [34].

Compression test specimens were fabricated only with the optimised parameters chosen from the tensile test under the following considerations. Firstly, the results produced within 25% compression range did not demonstrate sufficient sensitivity to identify any sound conclusion compared to the results from the tensile test and, secondly, the lattice structure designed with 2-3 mm feature size, which would be subject to the high impact load, should be fabricated only with the optimised parameters to gain maximum compression strength. As shown in Table 3 and Figure 4, the strength of parts built in X-axis and Z-axis are found to be very similar as opposed to the tensile parts fabricated in the same process conditions and thus the material can be considered isotropic under compression. It is also observed in Table 3 that the strength values of LP-15 W and NSE-2 built in both axes shows the similar values obtained by the part processed with LP-12 W and NSE-4. Since the increase in NSE increases the fabrication time the stress-strain dataset of LP-15 W and NSE- 2 is finally chosen as the optimised material characteristics and used in further FEA study.

4.3 Validity of computational data

The results reported in this research are directly comparable to existing literature documenting the kinematics of experimentally derived and computationally modelled head and helmet impact tests. Prange *et al.* reported the translational accelerations of the head recorded during experimental head drop tests performed with 1, 3 and 11 day old cadavers [35]. Mean peak translational accelerations, measured at the vertex of the head, were observed to be 47.7g and 81.4g for head drop test heights of 15cm (1.5ms^{-1}) and 30cm (2.9ms^{-1}), respectively [35]. Teng *et al.* experimentally determined the translational accelerations experienced by an EPS lined helmeted headform when impacted on a flat anvil at a velocity of 5.42ms^{-1} (in compliance with BS EN:1078 [12]), observing peak accelerations of approximately 180g [22]. This was computationally modelled to investigate the effects of novel inner liner designs on the translational accelerations experienced by the helmeted headform, with peak accelerations ranging between 172-405g across an extensive range of helmet design concepts, inner liner thicknesses and helmet impact locations [22]. The peak translational accelerations observed by this study were, however, reported between 10-36g at simulated impact test velocities of 2.2ms^{-1}. Given the paediatric cadaver heads were unhelmeted for the Prange *et al.* study and greater impact velocities were investigated in the Teng *et al.* study, the lower peak translational head accelerations acquired during this study appear comparable to the data collected during these experimental and computational modelling investigations.

4.4 Potential applications

This study is the first to establish the energy dissipating characteristics of lattice-based structures located in bicycle helmet inner liners, establishing that the density of the lattice structure influences the kinematics of the head during impact. Specifically, this research finds that a reduction in lattice structure density decreases the peak translational accelerations and increases the acceleration pulse durations experienced during impact, leading to the hypothesis that lattice-based structures appear to offer significant potential in the future design of safer bicycle helmets. Furthermore, this research identified that Flex, the novel rubber-like material evaluated in this study, was more effective for reducing peak translational accelerations and increasing pulse durations than the low density EPS material traditionally used in helmet inner liners.

With the strong association between head kinematics during impact and the severity of trauma [36], the ability of lattice structures to reduce peak translational accelerations and increase acceleration pulse durations represents a novel technique for improving the safety of bicycle helmet designs. The benefits of using

lattice-based structures for bicycle helmet designs do, however, extend beyond improving only helmet safety. Significant size, weight and material savings can be made when compared to traditional solid block designs, whilst incorporating novel lattice design concepts may reduce the rotational accelerations that are further experienced during oblique head impacts. The results from this research, therefore, provide strong evidence that lattice-based structures may play a vital role in the future development of innovative bicycle helmet design concepts. Prior to this, further research must be performed to determine the energy dissipating characteristics of lattice-based structures at a greater range of impact velocities; particularly for helmet impact test simulations that comply with British Standard recommendations (5.42ms^{-1} for a flat anvil and 4.57 ms^{-1} for a kerbstone anvil [12]).

5. Conclusions

This study reports the processing technique to produce Duraform® Flex with optimised material properties for use in attenuating the energy experienced during bicycle helmet impacts. Through the fabrication and testing of standardised tensile and compression specimens, the optimum process parameters established were a laser power of 15W, scanning exposure of 2 and a fixed power bed temperature of 155°C. Utilising these parameters, the effectiveness of lattice-based helmet inner liner designs in reducing head accelerations was investigated via a computational model. Results indicated that peak translational accelerations decreased with a reduction in lattice structure density, whilst acceleration pulse durations were increased. Furthermore, Flex was identified as being more effective for reducing peak translational accelerations and increasing pulse durations than the low density EPS material traditionally used in helmet inner liners experienced during impact. This study demonstrates that lattice-based inner liners, manufactured via additive manufacturing processes, have exciting potential towards improving bicycle helmet safety. Prior to this, the energy dissipating characteristics of lattice-based structures at a wider range of impact velocities must be investigated, whilst computational models must be experimentally validated through the fabrication and testing of bicycle helmets with optimised lattice-based inner liners.

References

[1]   Baker, SP, *et al*. Injuries to bicyclists: A national perspective. Johns Hopkins University Injury Prevention Center. (1993)

[2]   Bjornstig, U, *et al*. Head and face injuries to bicyclists with special reference to possible effects of helmet use. Journal of Trauma. Vol 33:6 (1992)

[3]   Ekman, R, *et al*. Can a combination of local, regional and national information substantially increase bicycle-helmet wearing and reduce

injuries? Experiences from Sweden. Accident Analysis & Prevention. Vol 29:3 (1997)

[4]   Friede, AM, *et al*. The epidemiology of injuries to bicycle riders. Pediatric Clinics of North America. Vol 32:1 (1985)

[5]   Thompson, RS, *et al*. A case-control study on the effectiveness of bicycle safety helmets. New England Journal of Medicine. Vol 320:21 (1989)

[6]   Sacks, JJ, *et al*. Bicycle associated head injuries and deaths in the United States from 1984 through 1988. How many are preventable? Journal of the American Medical Association. Vol 266:21 (1991)

[7]   Rivara, FP, *et al*. Prevention of bicycle-related injuries: helmets, education, and legislation. Annual review of public health. Vol 19:1 (1998)

[8]   Thompson, DC, *et al*. Helmets for preventing head and facial injuries in bicyclists. Cochrane Database of Systematic Reviews 4. (1999)

[9]   Moyes, SA. Changing pattern of child bicycle injury in the Bay of Plenty, New Zealand. Journal of paediatrics and child health. Vol 43:6 (2007)

[10]   Macpherson, A and Spinks, A. Cochrane review: Bicycle helmet legislation for the uptake of helmet use and prevention of head injuries. Evidence-Based Child Health: A Cochrane Review Journal. Vol 3:1 (2008)

[11]   World Health Organization. Helmets: A Road Safety Manual for Decision-makers and Practictioners. World Health Organization. (2006)

[12]   BS EN 1078:2012+A1:2012. Helmets for pedal cyclists and for users of skateboards and roller skates. British Standards Institution (BSI). (2012)

[13]   ASTM F1447 – 12. Standard Specification for Helmets Used in Recreational Bicycling or Roller Skating. ASTM International, West Conshohocken, PA. (2012)

[14]   Herlihy, D V. Bicycle: the history. New Haven: Yale University Press. p. 368. ISBN 978-0-300-12047-9. (2004)

[15]   Aare, M, *et al*. Injury tolerances for oblique impact helmet testing. International journal of crashworthiness. Vol 9:1 (2004).

[16]   ST CLAIR, VJ and Chinn BP. Assessment of current bicycle helmets for the potential to cause rotational injury. PUBLISHED PROJECT REPORT PPR213. (2007)

[17]   Rivara, FP, *et al*. Fit of bicycle safety helmets and risk of head injuries in children. Injury Prevention. Vol 5:3 (1999)

[18]   Halldin, P, *et al*. A new oblique impact test for motorcycle helmets. International Journal of Crashworthiness. Vol 6:1 (2001)

[19]   Alstin, T and Haupt A. SYSTEM AND METHOD FOR PROTECTING A BODYPART. European Patent No. EP 1947966. (2012)

[20]   Teng, T-L, *et al*. Development and validation of finite element model of helmet impact test. Proceedings of the Institution of Mechanical Engineers, Part L: Journal of Materials Design and Applications. Vol 227:1 (2013)

[21] Hansen, K, *et al*. Angular Impact Mitigation System for Bicycle Helmets to Reduce Head Acceleration and Risk of Traumatic Brain Injury. Accident Analysis & Prevention (2013).

[22] Teng, T-L, *et al*. Innovative design of bicycle helmet liners. Proceedings of the Institution of Mechanical Engineers, Part L: Journal of Materials Design and Applications (2013): 1464420713493590.

[23] Crookston, JJ, *et al*. Finite-element modelling of mechanical behaviour of rapid manufactured textiles, Proceedings of the Institution of Mechanical Engineers, Part L: Journal of Materials Design and Applications. Vol 222:1 (2008)

[24] Tan, JY, *et al*. Fabrication of channelled scaffolds with ordered array of micro-pores through microsphere leaching and indirect Rapid Prototyping technique. Biomedical Microdevices. Vol 15:1 (2013)

[25] Cerardi, A, *et al*. Mechanical characterization of polyamide cellular structures fabricated using selective laser sintering technologies. Materials & Design. Vol 46 (2013)

[26] Hooreweder, BV, *et al*. Microstructural characterization of SLS-PA12 specimens under dynamic tension/compression excitation. Polymer Testing. Vol 29:3 (2010)

[27] Dupin, S, *et al*. Microstructural origin of physical and mechanical properties of polyamide 12 processed by laser sintering. European Polymer Journal. Vol 48:9 (2012)

[28] Duraform® Flex Datasheet, 3D Systems. (2013)

[29] Rubber, vulcanized or thermoplastic — Determination of tensile stress-strain properties - BS ISO 37 (2011)

[30] Rubber, vulcanized or thermoplastic — Determination of compression stress-strain properties - BS ISO 7743 (2011)

[31] Ali, A, *et al*. A review of constitutive models for rubber-like materials. American Journal of Engineering and Applied Sciences. Vol 3:1 (2010)

[32] Texas Foam Inc. Expanded Polystyrene (EPS) Handbook. BASF Wyandotte Corporation. Accessed on 19/07/2013 at: http://www.texasfoam.com/EPS-Book.pdf

[33] Alwin, HZ. Development of a method to analyze structural insulated panels under transverse loading. Diss. Washington State University. (2002)

[34] Soe, S, *et al*. Mechanical characterisation of Duraform® Flex for FEA hyperelastic material modelling. Polymer Testing. Vol 34 (2014)

[35] Prange, MT, et al. Mechanical properties and anthropometry of the human infant head. Stapp car crash journal. Vol 48 (2004)

[36] Newman, J. A generalized acceleration model for brain injury threshold (GAMBIT). Proc. IRCOBI Conf. (1986)